AMERICAN SOCIETY FOR MICROBIOLOGY | mBio®

RESEARCH ARTICLE

The NOX Family of Proteins Is Also Present in Bacteria

Christine Hajjar,[a]* Mickaël V. Cherrier,[a] Gaëtan Dias Mirandela,[a]* Isabelle Petit-Hartlein,[a] Marie José Stasia,[b,c] Juan C. Fontecilla-Camps,[a] Franck Fieschi,[a] Jérôme Dupuy[a]

Univ. Grenoble Alpes, CEA, CNRS, IBS, 38000 Grenoble, France[a]; Univ. Grenoble Alpes, CNRS, TIMC-IMAG, 38000 Grenoble, France[b]; CDiRec, Pôle Biologie, CHU of Grenoble Alpes, Grenoble, France[c]

ABSTRACT Transmembrane NADPH oxidase (NOX) enzymes have been so far only characterized in eukaryotes. In most of these organisms, they reduce molecular oxygen to superoxide and, depending on the presence of additional domains, are called NOX or dual oxidases (DUOX). Reactive oxygen species (ROS), including superoxide, have been traditionally considered accidental toxic by-products of aerobic metabolism. However, during the last decade it has become evident that both $O_2^{\bullet-}$ and H_2O_2 are key players in complex signaling networks and defense. A well-studied example is the production of $O_2^{\bullet-}$ during the bactericidal respiratory burst of phagocytes; this production is catalyzed by NOX2. Here, we devised and applied a novel algorithm to search for additional *NOX* genes in genomic databases. This procedure allowed us to discover approximately 23% new sequences from bacteria (in relation to the number of NOX-related sequences identified by the authors) that we have added to the existing eukaryotic NOX family and have used to build an expanded phylogenetic tree. We cloned and overexpressed the identified *nox* gene from *Streptococcus pneumoniae* and confirmed that it codes for an NADPH oxidase. The membrane of the *S. pneumoniae* NOX protein (SpNOX) shares many properties with its eukaryotic counterparts, such as affinity for NADPH and flavin adenine dinucleotide, superoxide dismutase and diphenylene iodonium inhibition, cyanide resistance, oxygen consumption, and superoxide production. Traditionally, NOX enzymes in eukaryotes are related to functions linked to multicellularity. Thus, the discovery of a large family of NOX-related enzymes in the bacterial world brings up fascinating questions regarding their role in this new biological context.

IMPORTANCE NADPH oxidase (NOX) enzymes have not yet been reported in bacteria. Here, we carried out computational and experimental studies to provide the first characterization of a prokaryotic NOX. Out of 996 prokaryotic proteins showing NOX signatures, we initially selected, cloned, and overexpressed four of them. Subsequently, and based on preliminary testing, we concentrated our efforts on *Streptococcus* SpNOX, which shares many biochemical characteristics with NOX2, the referent model of NOX enzymes. Our work makes possible, for the first time, the study of pure forms of this important family of enzymes, allowing for biophysical and molecular characterization in an unprecedented way. Similar advances regarding other membrane protein families have led to new structures, further mechanistic studies, and the improvement of inhibitors. In addition, biological functions of these newly described bacterial enzymes will be certainly discovered in the near future.

KEYWORDS *Streptococcus pneumoniae*, biochemistry, electron transport, flavoenzymes, membrane proteins, metalloenzymes, oxidative stress, phylogenetic analysis

Received 17 August 2017 **Accepted** 27 September 2017 **Published** 7 November 2017

Citation Hajjar C, Cherrier MV, Dias Mirandela G, Petit-Hartlein I, Stasia MJ, Fontecilla-Camps JC, Fieschi F, Dupuy J. 2017. The NOX family of proteins is also present in bacteria. mBio 8:e01487-17. https://doi.org/10.1128/mBio.01487-17.

Editor Richard Gerald Brennan, Duke University School of Medicine

Address correspondence to Franck Fieschi, franck.fieschi@ibs.fr, or Jérôme Dupuy, jerome.dupuy@ibs.fr.

* Present address: Christine Hajjar, Centre d'Analyses et de Recherche UR EGP, Faculté des Sciences, Université Saint Joseph de Beyrouth, Beirut, Lebanon; Gaëtan Dias Mirandela, Strathclyde Institute of Pharmacy and Biomedical Sciences, Glasgow, United Kingdom.

Oxidative stress occurs when the balance between the generation of free radicals and their removal by antioxidants is lost. Free radicals are normally generated in the human body by metabolic processes, the best known being superoxide, peroxide, and radical hydroxyl oxygen species, which are collectively called reactive oxygen species (ROS). These species, which are highly reactive and can attack proteins, lipids, and nucleic acids, are major contributors to damage in biological organisms (1). These damages include aging-associated pathologies, cardiovascular disease, neurological disorders, fatty liver disease, cancers, and chronic inflammation (2). However, it is also apparent that ROS play essential roles in normal physiological processes, such as redox regulation, brain physiology, blood pressure, cell differentiation, hormone synthesis, and the very well-documented host defense system (3, 4). ROS-producing systems include xanthine oxidase, the mitochondrial respiratory chain, peroxidases, cytochrome P450 enzymes, uncoupled endothelial NO synthase, and phagocytic NADPH oxidases (NOXs). NOX proteins were the first identified systems that generate ROS not as a by-product but rather in a dedicated and targeted manner.

Eukaryotic NOXs are generally known to catalyze one-electron transmembrane transfer to molecular oxygen, resulting in the synthesis of superoxide anion, the initial ROS. Historically, gp91^{phox}, the NADPH oxidase from phagocytes and now called NOX2, was the first NOX described to produce ROS during the respiratory burst of the innate immunity process (5–10). Its first homolog was found in 1996 in rice (11), and within a few years five other NOXs were identified in mammals (6, 10, 12–17). The NOX family was subsequently divided into three subgroups, depending on the presence or absence of additional domains associated with the NOX2 protein core. They are widely distributed, tissue-specific modular proteins that share, for NOX1 to -4, a core consisting of a ferredoxin-NADP$^+$ reductase (FNR)–like domain (9) and a membrane-bound ferric reductase-like domain (FRD) called the YedZ domain in prokaryotes (18, 19) (Fig. 1A). They may also have, like NOX5, EF-hand domains and, in addition, as for dual oxidase 1 (DUOX1) and DUOX2, an amino-terminal peroxidase homology segment (3) (Fig. 1A). Besides NOX2, which is found in phagocytes, cardiac tissue and brain, where it is involved in host defense, muscle contraction, and neural degeneration, respectively (20), NOX enzymes from nonimmune tissues are involved in processes such as cell proliferation, apoptosis, and receptor signaling (3). Conversely, DUOX enzymes are implicated in reactions that involve extracellular matrix proteins, such as reactions for thyroid hormone synthesis (21, 22).

Blocking the undesirable actions of NOX enzymes is a strategy for treating oxidative stress-related pathologies and damage. In addition to ROS-provoked damage, deregulation of NOX-dependent ROS production can have pathological consequences related to a specific physiological context (e.g., chronic granulomatous disease, autoimmune disorders, hypothyroidism when ROS production is impaired, or cardiovascular and neurodegenerative diseases in the case of ROS overproduction) (21, 23).

Traditionally, the presence of NOX enzymes has been linked to functional requirements related to multicellularity (24). An exception is the yeasts *Saccharomyces cerevisiae* and *Schizosaccharomyces pombe*, which are unicellular organisms known to contain open reading frames (ORFs) homologous to NOX in its genome. However, except in one case (25), these ORFs have not been described as NOXs but as ferric reductases (FRE) (26). FRE and NOX enzymes have different final electron acceptors, O_2- and Fe^{3+}-chelating complexes, respectively, which are attributed to a few amino acid sequence changes within their FRD. Nevertheless, they have been traditionally placed within the same global protein family in phylogenetic analyses (18, 27). Although both FNR and YedZ, the model of bacterial FRD protein recently renamed MsrQ (18, 19, 28), are found separately in prokaryotes, the presence of functional *nox* genes in bacterial genomes containing both domains has not been established (29).

RESULTS

Computational screening of putative NOX sequences. An algorithm was devised to search for bacterial NOX sequences, using only the following essential eukaryotic

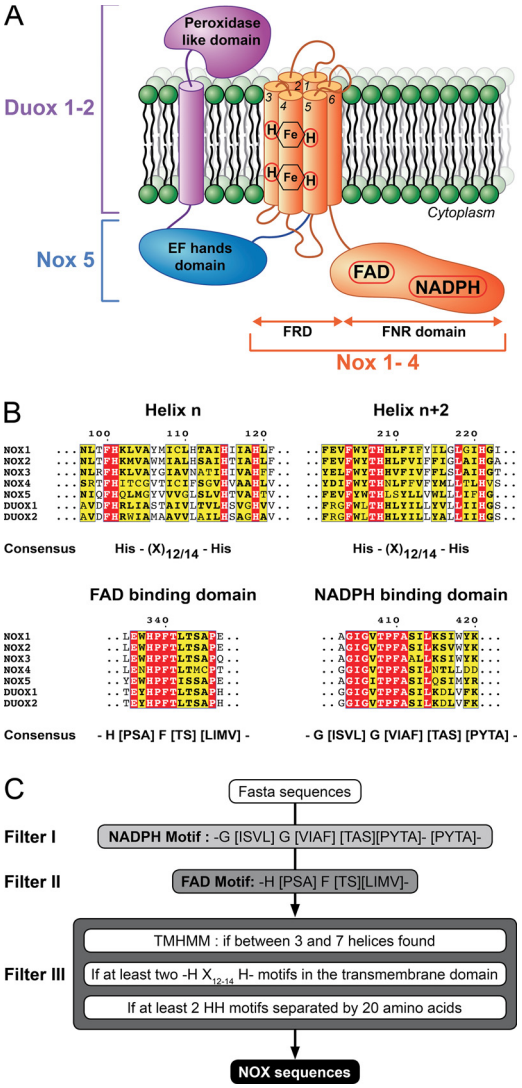

FIG 1 (A) Schematic representation of the NOX/DUOX protein family. (B) Multiple-sequence alignment of human NOX and DUOX proteins. Only the motifs used in this study are displayed. Amino acids strictly and partially conserved are highlighted in red and yellow, respectively. (C) Chart of the different filters used in this study to identify NOX sequences from Fasta formatted sequences. Each filter is independent and can be used separately.

motifs: (i) NADPH- and FAD-binding domains, both NOX specific, and (ii) two heme-binding His-$X_{12/14}$-His sequences (Fig. 1B). These filters were introduced to keep only sequences of proteins of interest for the next step. The final filter included the selection of *bis*-hystidyl patterns separated by at least 20 amino acids, which is the average length of a transmembrane α-helix, as well as a predicted transmembrane domain with at least three α-helices (Fig. 1C). The latter condition was used because the cytochrome *b*-like domain, which consists of six α-helices, is expected to bind the two-heme moieties at helices number 3 and 5. Starting from the 78,037,012 ORFs found in the UniprotKB/Swiss-Prot and UniProt/TrEMBL databases, our algorithm selected 4,404 putative NOX amino acid sequences from 1,492 different organisms, over a third of which were bacteria (Table 1). Conversely, only one archaeal sequence was found that fulfilled all of the above selection criteria (Fig. 1C). Subsequently, we selected a smaller set of sequences from all the represented domains of life (see Table S2 in the supplemental material) by removing (i) sequences from related organisms with >99% homology and (ii) a few sequences where the above motifs were not correctly aligned. Finally, 162 ORFs were selected to build an extended phylogenetic tree for the NOX/FRE

TABLE 1 Statistical analysis results from the search for NOX sequences in the UniProt database[a]

Data set	No. of sequences		
	Swiss-Prot	TrEMBL	Total
Total	553,474	77,483,538	78,037,012
Filter I (NADPH)	575	252,407	253,164
Filter II (FAD)	64	7,375	7,439
Filter III (HH)	47	4,357	4,404
Eukaryotes	47	3,354	3,401
Prokaryotes	0	996	996
Archaea	0	1	1
Unclassified	0	6	6

[a]The table shows the total number of sequences in the Swiss-Prot and TrEMBL databases, the number of sequences selected by the software after each filtering step, the number of eukaryotic, prokaryotic, and archaea sequences in each data set.

family (see Table S3 in the supplemental material). The tree (Fig. 2) shows a clear division between eukaryotes and prokaryotes, which may have evolutionary significance.

Selection of membrane protein candidates from bacterial genomes. In order to confirm that the sequences we extracted from bacterial genomes corresponded to functional NOX enzymes, we selected genes from *Acaryochloris marina*, *Escherichia coli*, *Pseudomonas aeruginosa*, and *Streptococcus pneumoniae* (AmNOX, EcNOX, PaNOX, and

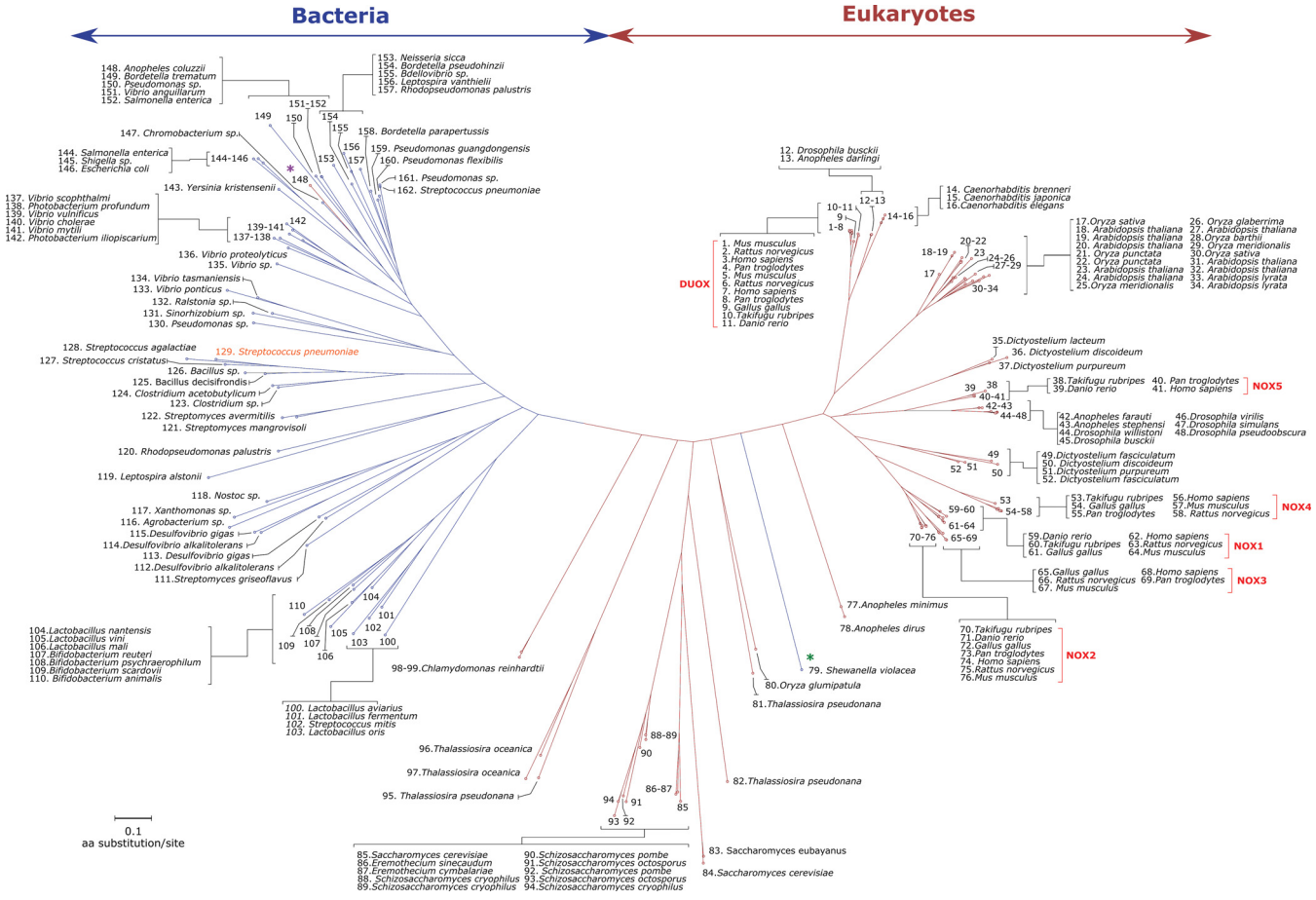

FIG 2 Phylogenetic tree of the NOX family. The tree was constructed using 162 sequences out of the 4,404 sequences identified in this study, and the sequences came from genera representative of all life domains (56). Eukaryote and prokaryote sequences are shown in red and blue, respectively. The green star highlights the only prokaryote sequence present in a eukaryote branch of the tree. The purple star highlights the unique eukaryote sequence present in the prokaryote branch of the tree. Each subfamily is indicated by blue square brackets. SpNOX is displayed in orange.

SpNOX, respectively) for further characterization. Their predicted protein topologies are very similar to the one calculated for NOX2, except for AmNOX, which is closer to NOX5 (Fig. S1). The selected genes were cloned and overexpressed in *E. coli* (Fig. S2), and the determination of the integrity of the resulting proteins was followed by spectrophotometry of the membrane extracts. Indeed, eukaryotic NOX enzymes are known to have a spectral signature with characteristic peaks at 426 nm and 558 nm in a difference (reduced minus oxidized) spectrum. The negative control was the same *E. coli* strain transformed by an expression plasmid devoid of a bacterial putative NOX gene. SpNOX, followed by PaNOX, were the proteins that showed the stronger spectroscopic signals (Fig. S3). Based on these results, we decided to pursue our study with SpNOX.

SpNOX exhibits a cytochrome b_{558} spectrum typical of NOX enzymes. SpNOX contained in the membrane preparation generated a spectrum similar to the one from NOX2. The dithionite-reduced difference spectrum showed a small peak at 558 nm, a shoulder at 530 nm, and a sharp peak at 426 nm (Fig. 3A) (30). As with many other cytochromes, the oxidized SpNOX gave a spectrum with a characteristic Soret band at 410 nm. The reduction of the heme *b* groups was followed by spectrophotometry, after the addition of NADPH. Increasing incubation times resulted in more pronounced peaks at 426 nm and 558 nm, while the spectrum decreased at 450 nm. These spectral changes indicate flavin reduction after electron transfer from NADPH (Fig. 3B) (31). Furthermore, heme reduction showed that electrons migrated from NADPH to the heme groups through the flavin cofactor, which is necessary to uncouple them (Fig. 3B).

SpNOX and NOX2 share enzymatic properties. A detergent screening was performed to identify the best-suited detergent to solubilize and stabilize SpNOX in an active form. The detergents of the maltoside family fulfilled all these requirements (Fig. S4). The His-tagged protein was found to be pure after its passage through a nickel affinity column followed by a size exclusion chromatographic step (Fig. S5). Next, the NADPH oxidase activity of the purified SpNOX was measured. It is well known that FAD is a required cofactor for the activity in eukaryotic NOX enzymes. Accordingly, the activity assay was performed with and without FAD, and superoxide production was determined by using a reporting system based on cytochrome *c* reduction. We found that purified SpNOX activity was dependent on FAD supplementation (Fig. 3C). However, the kinetic activity was strictly proportional to the final protein concentration, confirming that this activity is generated by an enzymatic process (Fig. S6A and B). SpNOX has lower affinities for NADPH and FAD (K_m of 8 μM and 0.13 μM) than NOX2 (K_m of 25 to 50 μM and 1 nM) (32, 33) (Fig. 3D and E) (34). It also exhibited a specific activity of 19 mol $O_2^{\bullet-}$/mol SpNOX/s, which represents 30% of that one reported for NOX2 (which is 64 mol $O_2^{\bullet-}$/mol cytochrome *b*/s [35]). Conversely, SpNOX has about twice the estimated specific activity of NOX4 (36). The stoichiometry of the reaction was established by simultaneously following substrate oxidation and cytochrome *c* reduction (Fig. 3F). One NADPH molecule should be able to transfer two electrons, ultimately producing two superoxide ions. From the kinetics presented in Fig. 3F, we obtained between 1.4 and 1.6 reduced cytochrome *c* molecules per oxidized NADPH molecule. This ratio compared well with the theoretical maximum value of 2, with the deficit explained by incomplete $O_2^{\bullet-}$ scavenging by cytochrome *c* (37, 38). Moreover, replacement of His heme ligands in the H69A-H129A and H83A-H142A variants resulted in membrane fractions displaying the same basal activity level as the membrane fraction of *E. coli* transformed with the empty expression vector (Fig. S6C and D). Thus, the NADPH oxidase activity observed in SpNOX depends on electron transfer through the hemes and, consequently, it is not due to electron loss at the SpNOX FNR domain.

A superoxide dismutation assay showed $O_2^{\bullet-}$ production by SpNOX. Superoxide production was also demonstrated by addition of superoxide dismutase (SOD) to the reaction mixture, which decreased cytochrome *c* reduction kinetics to 60% (Fig. 3G and H). The remaining SOD-insensitive activity (40%) likely resulted from direct cytochrome *c* reduction by SpNOX. Indeed, similar assays carried out under an argon atmosphere confirmed the direct electron transfer from SpNOX to cytochrome *c*, albeit

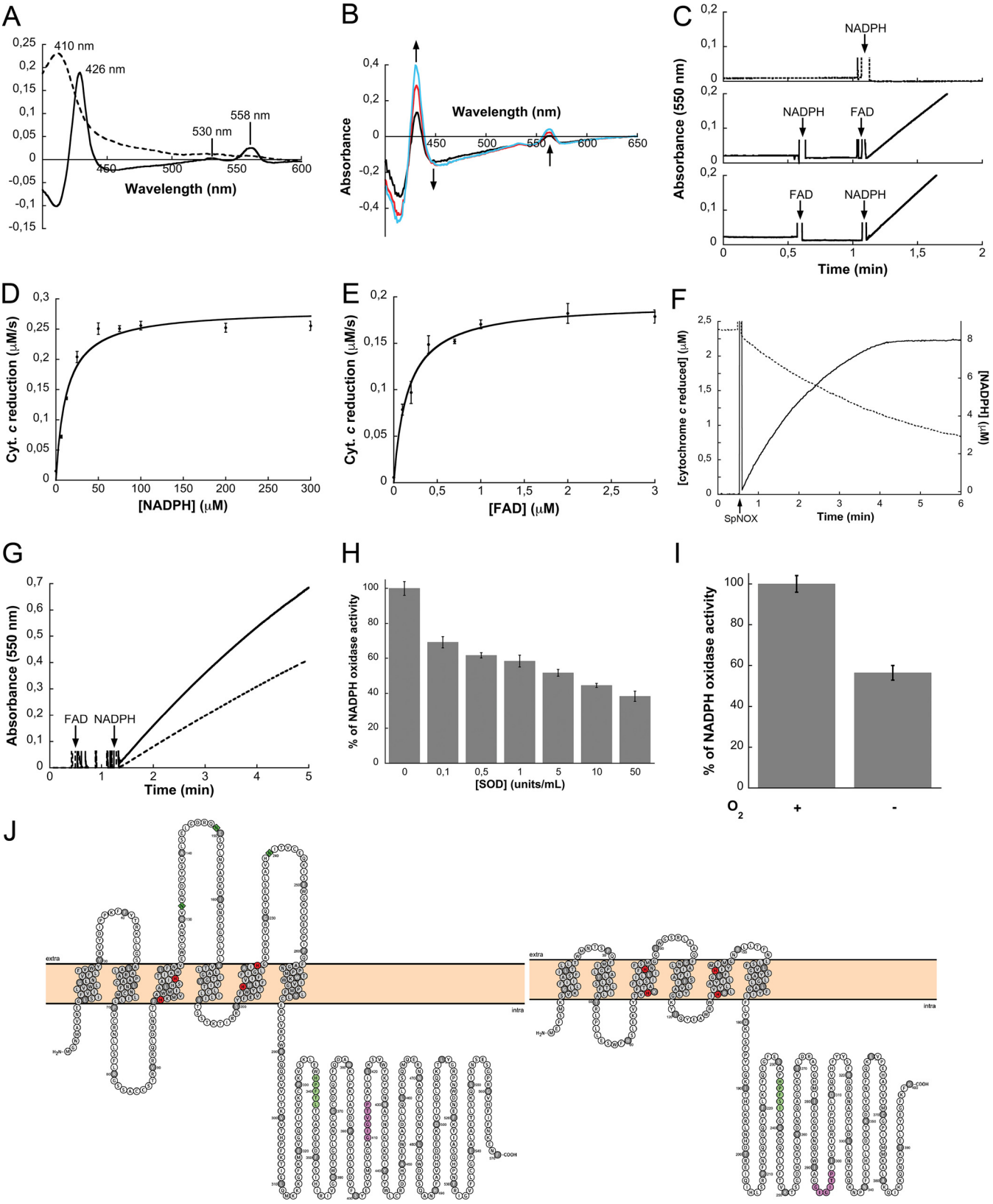

FIG 3 Enzymatic characterization of SpNOX. (A) Difference (reduced minus oxidized; solid line) and oxidized (dashed line) spectra from an *E. coli* membrane preparation expressing SpNOX. The typical peaks of NOX proteins are highlighted. (B) Absorbance spectra of a membrane preparation expressing SpNOX in the presence of 200 μM NADPH. Membrane reduction was sequentially recorded after 2 min (black line), 6 min (red line), and 10 min (blue line). Heme reduction was followed by an increase in peak height at 426 nm and 558 nm, showing that electrons can reach the membrane-bound core of SpNOX. (C) The activity of pure SpNOX was monitored in the presence or the absence of 2 μM FAD. (D and E) Michaelis-Menten saturation curves of SpNOX activity as a function of

(Continued on next page)

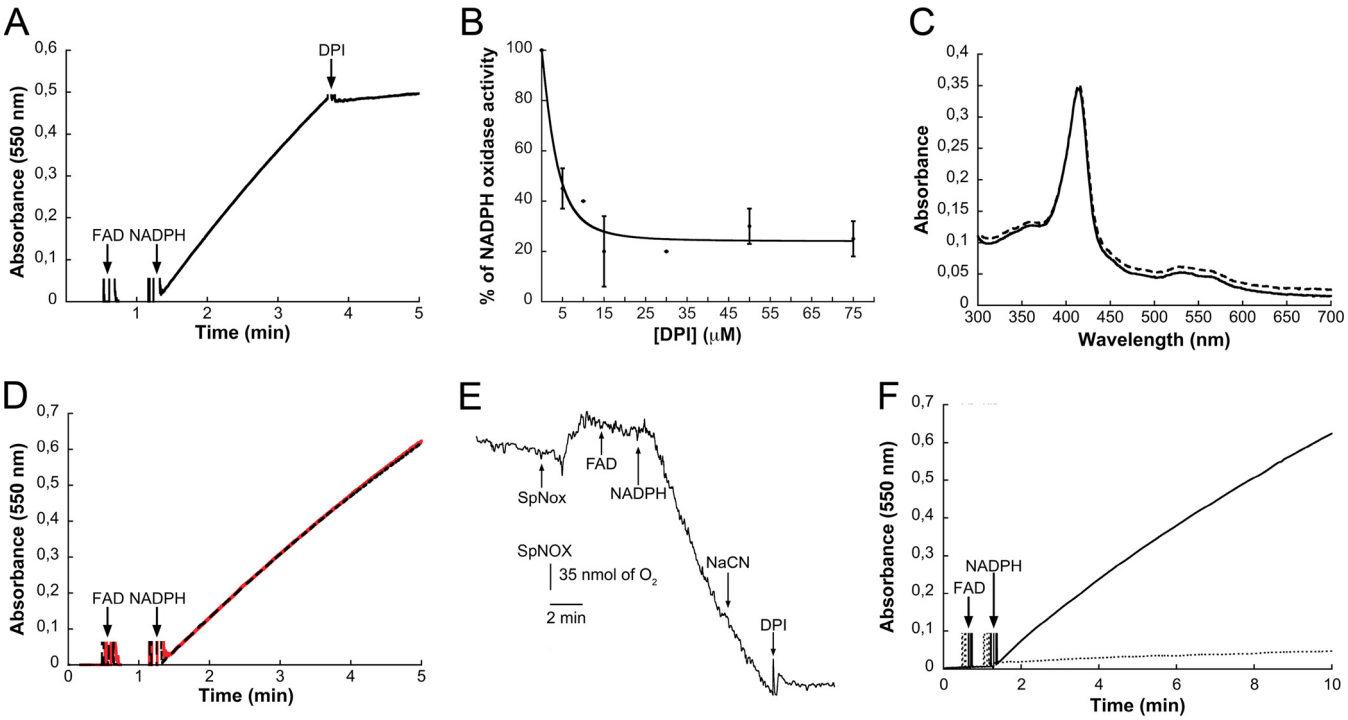

FIG 4 NOX activity of SpNOX. (A) SpNOX activities were measured after adding NADPH and FAD to final concentrations of 200 μM and 10 μM, respectively. The enzymatic activity was inhibited by the addition of 50 μM DPI (arrow). (B) Percentage of NADPH oxidase activity inhibition when monitored at different DPI concentrations. The error bars correspond to the standard deviations ($n = 3$). (C and D) Soret peak-containing spectra of SpNOX before (solid line) and after (dashed line) cyanide addition. As with eukaryotic NOXs, cyanide had no effect on the enzymatic activity of SpNOX. (E) Kinetics of cyanide-insensitive oxygen consumption by SpNOX. Only DPI inhibited this process. (F) The reduction of the ferric iron (dashed line) was inhibited by the addition of 0.4 mg/ml of SOD.

with lower efficiency (Fig. 3I). This result can be rationalized by comparing the topologies of NOX2 and SpNOX. The extracellular A, C, and E loops are significantly shorter in SpNOX than in NOX2. In the context of this *in vitro* assay, this topology difference may facilitate the access of cytochrome *c* to the external heme of SpNOX, closer to the extracellular side (Fig. 3J). Another possibility is the direct reduction by FAD, because both sides of SpNOX are accessible in the detergent-solubilized form of the protein.

Diphenylene iodonium inhibits SpNOX. DPI inhibits flavoenzymes such as NOX2 (36) and is widely used as a common inhibitor of NOX enzymes. The effect of DPI (39, 57) on SpNOX activity was evaluated in the cytochrome *c* reduction assay. Addition of DPI immediately stopped the reaction (Fig. 4A). This inhibitor reacts with reduced FAD to form a phenyl radical, which can either attack amino acids found at or near the FAD-binding site or directly attack the cofactor, ultimately resulting in irreversible enzyme inhibition (40). The calculated DPI 50% inhibitory concentration was around 5 μM for 1 μM FAD in our assay (Fig. 4B).

Cyanide does not inhibit SpNOX activity. Cyanide is known to be a global inhibitor of hemoproteins, thanks to its axial binding to the iron ion. In contrast to this general rule, NOX enzymes are insensitive to both azide and cyanide; this feature represents a hallmark of NOX proteins, where both hemes are expected to be hexacoordinated (6). We have also assessed this property for SpNOX by using catalase as a

FIG 3 Legend (Continued)
either NADPH concentration in the presence of 10 μM FAD (D) or FAD concentration in the presence of 200 μM NADPH (E). (F) NADPH oxidation (dashed line) and cytochrome *c* reduction (solid line) were followed simultaneously at 340 nm and 550 nm, respectively. (G) The reduction of cytochrome *c* (bold line) was inhibited by the addition of 0.3 mg/ml of SOD. (H) Inhibition effects of increasing SOD concentrations on SpNOX NADPH oxidase activity ($n = 5$). (I) SpNOX NADPH activity in either the presence (+) or absence (−) of O_2; this experiment was performed under argon. (J) The predicted NOX2 and SpNOX topologies consist of six transmembrane helices with 4 conserved histidines (red circles) in the transmembrane domain, NADPH-binding site (green circles), and FAD-binding site (purple circles). The NOX2 glycosylation sites are shown as green squares. Schemes were prepared using the Protter server (http://wlab.ethz.ch/protter/start/) and the topologies were predicted by the TMHMM server (http://www.cbs.dtu.dk/services/TMHMM/).

positive control. While cyanide incubation induced a shift of the 417 nm Soret band of catalase (data not shown), no modification was observed in the SpNOX spectrum upon NaCN addition (Fig. 4C). Furthermore, its NADPH oxidase activity was identical with or without added cyanide or azide (Fig. 4D). Finally, SpNOX-dependent oxygen consumption, measured using a Clark electrode (31) (Fig. 4E), confirmed its insensitivity to NaCN addition. Taken together, these data show that electrons transferred from NADPH to the heme groups through FAD can use molecular oxygen as the final acceptor. This activity, along with the DPI sensitivity and cyanide resistance described above, is indicative of the structural and functional relatedness of SpNOX to the eukaryotic NOX family of NADPH oxidases.

SpNOX is not a "true" ferric reductase. Within the global NOX/FRE family of enzymes harboring FRD and FNR domains, a distinction based on the final electron acceptor is often made between NOX/DUOX enzymes, which are capable of using oxygen as the electron acceptor, and FRE enzymes, which directly reduce the iron-chelating complex. In order to characterize further our bacterial NOX-related enzyme, we tested whether, in addition to its capacity to use oxygen as described above, SpNOX also had direct ferric reductase activity, as defined in a classical assay. We found that SpNOX was not able to reduce Fe^{3+} to Fe^{2+} in the presence of SOD (Fig. 4F). This showed that the observed ferric reductase activity of SpNOX is due to the produced superoxide ions that, in turn, are capable of reducing ferric iron. The specific activity was estimated to be 7.9 mol of Fe^{3+} reduced/mol of SpNOX/s, which represents 32% of NOX2's ferric reductase activity. Indeed, the same experiment was performed using the human cytochrome b_{558}, for which the specific activity was calculated to be 24 mol of Fe^{3+} reduced/mol of cytochrome *b*/s (data not shown). The SpNOX to NOX2 ratios of NADPH oxidase activity and ferric reductase activity were comparable, as expected from the dependency of the latter on the production of $O_2^{\bullet -}$ by the former. Thus, within the NOX/FRE family of enzymes, SpNOX appears to be more related to a NOX than to a FRE, as indicated by its *in vitro* reactivity.

DISCUSSION

Although new members of the NOX family of electron transfer membrane proteins have been continuously discovered since the 2000s, they have been restricted to eukaryotic organisms, from fungi to animals and plants. In 2004, a first indication of an evolutionary relationship of NOX enzymes with prokaryotic proteins was suggested by the simultaneous description by Von Rozycki et al. (19) and Sanchez-Pulido et al. (27) of the bacterial MsrQ protein. MsrQ was described as an FRD involved in electron transfer and significantly homologous to the membranous moiety of eukaryotic NOX proteins. Along the same lines, we reported recently that the flavin reductase Fre could be the potential electron donor to MsrQ. Thus, these two proteins mimic the architectural organization of eukaryotic NOX (38). This may be considered an intermediate evolutionary organization, ancestral to the eukaryotic NOX, where FRD and FNR domains are fused into a single polypeptide chain (38). The work presented here goes far beyond preliminary reports (19, 27), because we provide the first evidence for the existence of a large family of prokaryotic membrane proteins that have all the sequence motifs and predicted topological characteristics of NOX-related enzymes. All these prokaryotic sequences are well separated from their eukaryotic counterparts in the phylogenetic tree (Fig. 2). This suggests that they constitute a new subgroup in the NOX family of enzymes. A few bacterial sequences are located in the eukaryotic branches of the tree. These NOX5-like sequences, found, for instance, in *Acaryochloris marina*, were probably horizontally transferred from eukaryotic genomes (18). Moreover, there is one eukaryotic sequence from *Anapheles coluzzii* present in the middle of the bacteria subgroup. This sequence is very close to that in *Chromobacterium* sp., which is a bacterium that can effectively colonize the intestines of *A. coluzzii* (41). The horizontal gene transfer between bacteria and animals is still controversial and in this particular case it could have resulted from contamination during genome sequencing (42, 43). Thus, with the combinatorial use of specific sequence motifs characteristic of

NOX enzymes, we have been able to identify a large number of bacterial sequences having (i) six transmembrane helices with (ii) conserved bis-histidyl motifs within the third and fifth transmembrane helices and (iii) a C-terminal dehydrogenase region containing FAD- and NADPH-binding domains.

This bioinformatics study was complemented with a biochemical characterization of the representative bacterial SpNOX, which fully confirmed its close functional and structural relationship with the eukaryotic NOX enzymes. Indeed, both systems are able to use NADPH as an electron donor and oxygen as the final acceptor. As expected, we also found that electron transfer from NADPH to O_2 requires FAD and heme cofactors. Furthermore, like well-described NOX proteins, SpNOX is both sensitive to the DPI inhibitor, which targets the FAD moiety, and insensitive to cyanide.

In spite of the many common features, there are some clear differences between SpNOX and mammalian NOXs. Indeed, in contrast to NOX1 to -4, SpNOX does not need a p22^{phox}-like subunit for proper membrane integration. Moreover, the purified recombinant form of the protein is constitutively active *in vitro*, without requiring cytosolic factors or an activation process. Also, SpNOX is active in a detergent-solubilized form, which is not the case for the mammalian NOX enzymes, which need to be reconstituted in a lipid bilayer (35, 44). Indeed, in order to be active, NOX2 needs to be reconstituted in a membrane forming a complex with cytosolic factors, lipid polar heads, and phosphatidylinositol, which is the template for p47^{phox} binding and global assembly (45). Being independent from such an assembly process, SpNOX is fully functional when inserted in a detergent micelle. Thus, all in all, we believe that SpNOX is a good model to study the activated state of a mammalian NOX2-like enzyme. The recombinant production of SpNOX will allow for novel biophysical and biochemical studies of NOX-related membrane-bound enzymes.

Importantly, the presence of these enzymes in prokaryotes raises the question of what could be their function. The recent emergence of ROS as signaling molecules in eukaryotes has led to the concept of ROS signaling within and between cells (4, 20). An example of cross-cell communication is given by the slime mold *Dictyostelium discoideum*. Although it grows as a single amoeba when food is available, when starved the single cells aggregate, constituting a multicellular organism of up to a million amoebae, which forms a fruiting body that sporulates (46). The aggregate does not form if $O_2^{\bullet-}$ is scavenged either pharmacologically or by overexpression of SOD (46). Bloomfield et al. suggested that this ($O_2^{\bullet-}$)-based signaling mechanism arose early in the evolution of multicellular organisms and most likely relies on NOXs, which genes are present in *Dictyostelium* (14) (Fig. 2). Indeed, Lardy et al. demonstrated the central role of NOX homologs in different phases of development of the slime mold (47).

Until now, it has been accepted that bacterial ROS production depends on reactions that are not primarily intended for that purpose. This apparent opportunistic, or even accidental, use of ROS appears to be in stark contrast with the regulated $O_2^{\bullet-}$ production by NOX and its possible transformation to H_2O_2 by SOD found in eukaryotes (2). Indeed, regulated ROS production is expected to be amenable to modulate intercellular signaling in a well-defined spatiotemporal context. In this context, our discovery that NOX-related enzymes are also present in bacteria (Fig. 2) is especially intriguing. Although, as far as we can tell, highly regulated generation of ROS in these microorganisms has not been reported, our results suggest that such process could be biologically important, for instance, for biofilm formation and dynamics. Indeed, bacterial biofilms, which are now known to be the most common way for bacteria to thrive in nature, have been considered an example of multicellularity (48). The use of NOX by bacterial communities could be a means to communicate within biofilms, as occurs in eukaryotes when $O_2^{\bullet-}$ is generated in processes such as protozoan cell aggregation or to mediate, along with H_2O_2, the many other ROS-dependent signaling processes known to take place in metazoans.

An alternative possibility is that, although our bioinformatics and biochemical analyses indicated that SpNOX is a bona fide "NADPH oxidase," it may not necessarily function, in its bacterial physiological context, as the eukaryotic NOXs do. For instance,

bacterial NOX-like proteins may be components of electron transfer pathways where O_2 is not the physiological electron acceptor. A recent example of such a possibility is the discovery that MsrQ transfers its electrons to MsrP, a molybdopterin protein acceptor present in the periplasm of *E. coli*, to catalyze the reduction of methionine sulfoxide in oxidatively damaged periplasmic proteins (49). The observation that SpNOX can directly reduce cytochrome *c* demonstrates that its more exposed heme is accessible to potential periplasmic redox partners. This provides some support to the hypothesis of alternative electron acceptors for bacterial NOX proteins in general. We conclude that many new and unanticipated functions and synthetic pathways may turn out to be associated with this new family of bacterial NOX.

An SpNOX knockout of *S. pneumoniae* did not display an identifiable phenotype (data not shown). It is clear that further studies will be required to address the role of bacterial NOX in signaling and/or metabolic processes, as postulated above.

In conclusion, the work reported here has allowed us to identify for the first time, both theoretically and functionally, a significant number of bacterial protein sequences that are found in current databases and are counterparts of eukaryotic NOX proteins.

MATERIALS AND METHODS

NOX sequence identification. The software used to identify NOX sequences in bacterial genomes was written in Python 3.0. The program used three filters. The first two filters selected sequences containing H(PSA)F[TS][LIMV] (FAD-binding motif) and G(ISVL)G[VIAF][TAS][PYTA] (NADPH-binding motifs) (Fig. 1), defined using the 101 protein sequences identified by Kawahara et al. (50). The third filter selected sequences that contained the four histidine residues responsible for coordinating the two-heme moieties of the cytochrome *b*-like motif. The TMHMM sequence (51) was used to locate transmembrane α-helices. Sequences with more than seven predicted α-helices (the number found in DUOX1 and -2) were rejected, whereas sequences with at least 3 predicted α-helices were kept to account for errors in the prediction.

Amino acid sequence alignments and phylogenetic tree construction. Multiple sequence alignment of NOX sequences was carried out with Clustal Omega (52). The tree was built from 162 putative NOX sequences (Table S3) by using PhyML 3.0. The sequences used for software validation are provided in Table S1.

Cloning of the bacterial *nox* genes in a pQLink N vector. Genes were optimized for expression in *E. coli* and synthetized via GenScript. They were inserted in a pUC57 vector conferring ampicillin resistance and providing a His tag coding sequence in frame with the 5′ end of the inserted gene. The pUC57 vectors containing the bacterial *nox* genes were treated with Not1 and BamHI restriction enzymes for 2 h at 37°C and ligated to a NotI-BamHI-digested pQLink N vector to yield pQLink N-bacterial NOX expression plasmids. Several expression strains were tested, and the best result was obtained with BL21(DE3) pLysS expression cells.

SpNOX expression and purification. The culture was grown in LB medium containing chloramphenicol (0.034mg/ml) and ampicillin (0.1 mg/ml) at 37°C with shaking. At an optical density at 600 nm of 1.5, isopropyl-β-D-thiogalactopyanoside (IPTG) was added to a final concentration of 0.1 mM with shaking at 210 rpm to induce the expression of the protein of interest. After 4 h of induction, cells were harvested by centrifugation (7,000 $\times$ *g*, 30 min, 4°C).

The culture pellet was resuspended in 50 mM Tris-HCl (pH 7), 250 mM NaCl, 10% glycerol supplemented with DNase and an antiprotease cocktail. Cells were disrupted using a microfluidizer (M-1105; Microfluidics, USA) at 1,400 lb/in^2 (4 to 5 passes). Unbroken cells, debris, and inclusion bodies were removed by one low-speed centrifugation step at 8,000 $\times$ *g* in a Beckman rotor 850 followed by ultracentrifugation at 235,000 $\times$ *g* (Beckman Ti-45 rotor at 45,000 rpm) for 45 min at 4°C. The resulting pellet of membranes was solubilized to 2 mg/ml in 50 mM Tris-HCl (pH 7), 300 mM NaCl, and 5 mM (0.5%) lauryl maltose neopentyl glycol (NG310-MNG). Equilibrated Ni-nitrilotriacetic acid (NTA)–Sepharose resin was added to the mixture (1 ml per 15 mg of protein) and incubated overnight with shaking at 4°C.

Loaded resin was packed in a gravity column and washed thoroughly with Tris-HCl buffer (pH 7), 300 mM NaCl, 0.015% MNG, and 50 mM imidazole. The same buffer supplied with 300 mM imidazole was used to elute the protein. Pure fractions were concentrated and loaded on a Superdex 200 column previously equilibrated with Tris buffer (pH 7.0), 300 mM NaCl, and 0.003% MNG. The protein sample was stored at 4°C.

Spectroscopy signatures. Differential (reduced minus oxidized) spectra were recorded between 600 and 400 nm using a Cary 50 Bio UV/visible spectrophotometer (6). Reaction mixtures (total volume of 130 μl in quartz cuvettes) consisted of membranes at 1 mg/ml. The spectrum of reduced protein was obtained after adding a few crystals of sodium dithionite.

NADPH oxidase activity assay. NADPH oxidase activity was assayed by following the reduction of cytochrome *c* (58). NADPH and FAD were added to 0.1 μg of protein to final concentrations up to 200 μM and 10 μM, respectively; the extent of cytochrome *c* (100 μM) reduction was calculated based on the absorbance difference at 550 nm with an absorption coefficient of 21,000 M^{-1} cm^{-1}. DPI was added to a final concentration of 50 μM. Adding 10 units of superoxide dismutase verified the specificity of the product.

Measurement of cyanide-resistant oxygen consumption. The oxygen consumption rate of 20 μg of purified SpNOX was measured by using a Clark electrode in a final volume of 1.6 ml. The oxygraph was calibrated by addition of dithionite to air-saturated buffer to establish the zero level of O_2 concentration. Sodium cyanide and DPI were added at final concentrations of 1 mM and 50 μM, respectively (54).

Ferric reductase activity assay. Ferrous ions form a complex with ferrozine, which can be monitored at 562 nm. The Fe-NTA solution was prepared as described by Awai et al. (55). The ferrozine stock solution was prepared in 150 mM of acetate buffer (pH 7) to a final concentration of 100 mM. Ferric reduction was calculated based on the absorbance difference at 562 nm, using an absorption coefficient of 28,000 M^{-1} cm^{-1} (53). The reaction mixture consisted of 0.1 μg/ml SpNOX, 0.4 mM ferrozine, 0.3 mM Fe-NTA, and 10 μM FAD, with the addition of 200 μM NADPH to a final volume of 1 ml to start the reaction.

SUPPLEMENTAL MATERIAL

Supplemental material for this article may be found at https://doi.org/10.1128/mBio.01487-17.

FIG S1, JPG file, 2.7 MB.
FIG S2, JPG file, 2 MB.
FIG S3, JPG file, 0.7 MB.
FIG S4, JPG file, 1 MB.
FIG S5, JPG file, 1.1 MB.
FIG S6, JPG file, 1.5 MB.
TABLE S1, DOCX file, 0.03 MB.
TABLE S2, DOCX file, 0.03 MB.
TABLE S3, DOCX file, 0.04 MB.

ACKNOWLEDGMENTS

We are grateful to A. Picciocchi for his comments on an earlier version of the manuscript and C. Durmort for her help with the SpNOX knockout, and we thank Charlotte Genestet for technical help. This work used the platforms of the Grenoble Instruct Center (ISBG; UMS 3518 CNRS-CEA-UGA-EMBL) and notably the MP3 platform, with support from FRISBI (ANR-10-INSB-05-02) and GRAL (ANR-10-LABX-49-01) within the Grenoble Partnership for Structural Biology.

This work has been supported by a grant from the Joseph Fourier University (AGIR 2013—Grenoble, France). We also acknowledge support from the French Agence Nationale de la Recherche (ANR), under contract ANR-2010-1536-01 (Prototype Nox) and to the Programme Technology pour la Santé du CEA under contract A-TSANV-03-26 (BOSS).

REFERENCES

1. D'Autréaux B, Toledano MB. 2007. ROS as signalling molecules: mechanisms that generate specificity in ROS homeostasis. Nat Rev Mol Cell Biol 8:813–824. https://doi.org/10.1038/nrm2256.
2. Nathan C, Cunningham-Bussel A. 2013. Beyond oxidative stress: an immunologist's guide to reactive oxygen species. Nat Rev Immunol 13:349–361. https://doi.org/10.1038/nri3423.
3. Lambeth JD. 2004. NOX enzymes and the biology of reactive oxygen. Nat Rev Immunol 4:181–189. https://doi.org/10.1038/nri1312.
4. Mittler R, Vanderauwera S, Suzuki N, Miller G, Tognetti VB, Vandepoele K, Gollery M, Shulaev V, Van Breusegem F. 2011. ROS signaling: the new wave? Trends Plant Sci 16:300–309. https://doi.org/10.1016/j.tplants.2011.03.007.
5. Babior BM, Kipnes RS, Curnutte JT. 1973. Biological defense mechanisms. The production by leukocytes of superoxide, a potential bactericidal agent. J Clin Invest 52:741–744. https://doi.org/10.1172/JCI107236.
6. Babior BM, Curnutte JT, Kipnes BS. 1975. Pyridine nucleotide-dependent superoxide production by a cell-free system from human granulocytes. J Clin Invest 56:1035–1042. https://doi.org/10.1172/JCI108150.
7. Segal AW, Jones OT. 1978. Novel cytochrome *b* system in phagocytic vacuoles of human granulocytes. Nature 276:515–517. https://doi.org/10.1038/276515a0.
8. Royer-Pokora B, Kunkel LM, Monaco AP, Goff SC, Newburger PE, Baehner RL, Cole FS, Curnutte JT, Orkin SH. 1986. Cloning the gene for an inherited human disorder—chronic granulomatous disease—on the basis of its chromosomal location. Nature 322:32–38. https://doi.org/10.1038/322032a0.
9. Rotrosen D, Yeung CL, Leto TL, Malech HL, Kwong CH. 1992. Cytochrome b558: the flavin-binding component of the phagocyte NADPH oxidase. Science 256:1459–1462. https://doi.org/10.1126/science.1318579.
10. Clark RA. 1999. Activation of the neutrophil respiratory burst oxidase. J Infect Dis 179(Suppl 2):S309–S317. https://doi.org/10.1086/513849.
11. Groom QJ, Torres MA, Fordham-Skelton AP, Hammond-Kosack KE, Robinson NJ, Jones JD. 1996. rbohA, a rice homologue of the mammalian gp91phox respiratory burst oxidase gene. Plant J 10:515–522. https://doi.org/10.1046/j.1365-313X.1996.10030515.x.
12. Bánfi B, Molnár G, Maturana A, Steger K, Hegedûs B, Demaurex N, Krause KH. 2001. A Ca(2+)-activated NADPH oxidase in testis, spleen, and lymph nodes. J Biol Chem 276:37594–37601. https://doi.org/10.1074/jbc.M103034200.
13. Cheng G, Cao Z, Xu X, van Meir EG, Lambeth JD. 2001. Homologs of gp91phox: cloning and tissue expression of Nox3, Nox4, and Nox5. Gene 269:131–140. https://doi.org/10.1016/S0378-1119(01)00449-8.
14. Edens WA, Sharling L, Cheng G, Shapira R, Kinkade JM, Lee T, Edens HA, Tang X, Sullards C, Flaherty DB, Benian GM, Lambeth JD. 2001. Tyrosine cross-linking of extracellular matrix is catalyzed by Duox, a multidomain oxidase/peroxidase with homology to the phagocyte oxidase subunit gp91phox. J Cell Biol 154:879–891. https://doi.org/10.1083/jcb.200103132.
15. Geiszt M, Kopp JB, Várnai P, Leto TL. 2000. Identification of renox, an

NAD(P)H oxidase in kidney. Proc Natl Acad Sci U S A 97:8010–8014. https://doi.org/10.1073/pnas.130135897.
16. Lambeth JD, Cheng G, Arnold RS, Edens WA. 2000. Novel homologs of gp91phox. Trends Biochem Sci 25:459–461. https://doi.org/10.1016/S0968-0004(00)01658-3.
17. Suh YA, Arnold RS, Lassegue B, Shi J, Xu X, Sorescu D, Chung AB, Griendling KK, Lambeth JD. 1999. Cell transformation by the superoxide-generating oxidase Mox1. Nature 401:79–82. https://doi.org/10.1038/43459.
18. Zhang X, Krause KH, Xenarios I, Soldati T, Boeckmann B. 2013. Evolution of the ferric reductase domain (FRD) superfamily: modularity, functional diversification, and signature motifs. PLoS One 8:e58126. https://doi.org/10.1371/journal.pone.0058126.
19. von Rozycki T, Yen MR, Lende EE, Saier MH. 2004. The YedZ family: possible heme binding proteins that can be fused to transporters and electron carriers. J Mol Microbiol Biotechnol 8:129–140. https://doi.org/10.1159/000085786.
20. Prosser BL, Ward CW, Lederer WJ. 2011. X-ROS signaling: rapid mechano-chemo transduction in heart. Science 333:1440–1445. https://doi.org/10.1126/science.1202768.
21. O'Neill S, Brault J, Stasia MJ, Knaus UG. 2015. Genetic disorders coupled to ROS deficiency. Redox Biol 6:135–156. https://doi.org/10.1016/j.redox.2015.07.009.
22. De Deken X, Wang D, Many MC, Costagliola S, Libert F, Vassart G, Dumont JE, Miot F. 2000. Cloning of two human thyroid cDNAs encoding new members of the NADPH oxidase family. J Biol Chem 275:23227–23233. https://doi.org/10.1074/jbc.M000916200.
23. Bedard K, Krause KH. 2007. The NOX family of ROS-generating NADPH oxidases: physiology and pathophysiology. Physiol Rev 87:245–313. https://doi.org/10.1152/physrev.00044.2005.
24. Bedard K, Lardy B, Krause KH. 2007. NOX family NADPH oxidases: not just in mammals. Biochimie 89:1107–1112. https://doi.org/10.1016/j.biochi.2007.01.012.
25. Rinnerthaler M, Büttner S, Laun P, Heeren G, Felder TK, Klinger H, Weinberger M, Stolze K, Grousl T, Hasek J, Benada O, Frydlova I, Klocker A, Simon-Nobbe B, Jansko B, Breitenbach-Koller H, Eisenberg T, Gourlay CW, Madeo F, Burhans WC, Breitenbach M. 2012. Yno1p/Aim14p, a NADPH-oxidase ortholog, controls extramitochondrial reactive oxygen species generation, apoptosis, and actin cable formation in yeast. Proc Natl Acad Sci U S A 109:8658–8663. https://doi.org/10.1073/pnas.1201629109.
26. Georgatsou E, Alexandraki D. 1994. Two distinctly regulated genes are required for ferric reduction, the first step of iron uptake in Saccharomyces cerevisiae. Mol Cell Biol 14:3065–3073. https://doi.org/10.1128/MCB.14.5.3065.
27. Sanchez-Pulido L, Rojas AM, Valencia A, Martinez-A C, Andrade MA. 2004. ACRATA: a novel electron transfer domain associated to apoptosis and cancer. BMC Cancer 4:98. https://doi.org/10.1186/1471-2407-4-98.
28. Roman DG, Dancis A, Anderson GJ, Klausner RD. 1993. The fission yeast ferric reductase gene frp1+ is required for ferric iron uptake and encodes a protein that is homologous to the gp91-phox subunit of the human NADPH phagocyte oxidoreductase. Mol Cell Biol 13:4342–4350. https://doi.org/10.1128/MCB.13.7.4342.
29. Sumimoto H. 2008. Structure, regulation and evolution of Nox-family NADPH oxidases that produce reactive oxygen species. FEBS J 275:3249–3277. https://doi.org/10.1111/j.1742-4658.2008.06488.x.
30. Pember SO, Heyl BL, Kinkade JM, Lambeth JD. 1984. Cytochrome b558 from (bovine) granulocytes. Partial purification from Triton X-114 extracts and properties of the isolated cytochrome. J Biol Chem 259:10590–10595.
31. Cross AR, Parkinson JF, Jones OT. 1984. The superoxide-generating oxidase of leucocytes. NADPH-dependent reduction of flavin and cytochrome *b* in solubilized preparations. Biochem J 223:337–344. https://doi.org/10.1042/bj2230337.
32. Clark RA, Leidal KG, Pearson DW, Nauseef WM. 1987. NADPH oxidase of human neutrophils. Subcellular localization and characterization of an arachidonate-activatable superoxide-generating system. J Biol Chem 262:4065–4074.
33. Nozaki M, Takeshige K, Sumimoto H, Minakami S. 1990. Reconstitution of the partially purified membrane component of the superoxide-generating NADPH oxidase of pig neutrophils with phospholipid. Eur J Biochem 187:335–340. https://doi.org/10.1111/j.1432-1033.1990.tb15310.x.
34. Hashida S, Yuzawa S, Suzuki NN, Fujioka Y, Takikawa T, Sumimoto H, Inagaki F, Fujii H. 2004. Binding of FAD to cytochrome b558 is facilitated during activation of the phagocyte NADPH oxidase, leading to superoxide production. J Biol Chem 279:26378–26386. https://doi.org/10.1074/jbc.M309724200.
35. Lord CI, Riesselman MH, Gripentrog JM, Burritt JB, Jesaitis AJ, Taylor RM. 2008. Single-step immunoaffinity purification and functional reconstitution of human phagocyte flavocytochrome b. J Immunol Methods 329:201–207. https://doi.org/10.1016/j.jim.2007.10.008.
36. Nisimoto Y, Diebold BA, Cosentino-Gomes D, Constentino-Gomes D, Lambeth JD. 2014. Nox4: a hydrogen peroxide-generating oxygen sensor. Biochemistry 53:5111–5120. https://doi.org/10.1021/bi500331y.
37. Rieske JS. 1967. The quantitative determination of mitochondrial hemoproteins. Methods Enzymol 10:488–493.
38. Juillan-Binard C, Picciocchi A, Andrieu JP, Dupuy J, Petit-Hartlein I, Caux-Thang C, Vivès C, Nivière V, Fieschi F. 2017. A two-component NADPH oxidase (NOX)-like system in bacteria is involved in the electron transfer chain to the methionine sulfoxide reductase MsrP. J Biol Chem 292:2485–2494. https://doi.org/10.1074/jbc.M116.752014.
39. Ellis JA, Mayer SJ, Jones OT. 1988. The effect of the NADPH oxidase inhibitor diphenyleneiodonium on aerobic and anaerobic microbicidal activities of human neutrophils. Biochem J 251:887–891. https://doi.org/10.1042/bj2510887.
40. O'Donnell VB, Smith GC, Jones OT. 1994. Involvement of phenyl radicals in iodonium inhibition of flavoenzymes. Mol Pharmacol 46:778–785.
41. Ramirez JL, Short SM, Bahia AC, Saraiva RG, Dong Y, Kang S, Tripathi A, Mlambo G, Dimopoulos G. 2014. Chromobacterium Csp_P reduces malaria and dengue infection in vector mosquitoes and has entomopathogenic and in vitro anti-pathogen activities. PLoS Pathog 10:e1004398. https://doi.org/10.1371/journal.ppat.1004398.
42. Dunning Hotopp JC. 2011. Horizontal gene transfer between bacteria and animals. Trends Genet 27:157–163. https://doi.org/10.1016/j.tig.2011.01.005.
43. Ku C, Martin WF. 2016. A natural barrier to lateral gene transfer from prokaryotes to eukaryotes revealed from genomes: the 70 % rule. BMC Biol 14:89. https://doi.org/10.1186/s12915-016-0315-9.
44. Taylor RM, Burritt JB, Foubert TR, Snodgrass MA, Stone KC, Baniulis D, Gripentrog JM, Lord C, Jesaitis AJ. 2003. Single-step immunoaffinity purification and characterization of dodecylmaltoside-solubilized human neutrophil flavocytochrome b. Biochim Biophys Acta 1612:65–75. https://doi.org/10.1016/S0005-2736(03)00086-5.
45. Mizrahi A, Berdichevsky Y, Ugolev Y, Molshanski-Mor S, Nakash Y, Dahan I, Alloul N, Gorzalczany Y, Sarfstein R, Hirshberg M, Pick E. 2006. Assembly of the phagocyte NADPH oxidase complex: chimeric constructs derived from the cytosolic components as tools for exploring structure-function relationships. J Leukoc Biol 79:881–895. https://doi.org/10.1189/jlb.1005553.
46. Bloomfield G, Pears C. 2003. Superoxide signalling required for multicellular development of Dictyostelium. J Cell Sci 116:3387–3397. https://doi.org/10.1242/jcs.00649.
47. Lardy B, Bof M, Aubry L, Paclet MH, Morel F, Satre M, Klein G. 2005. NADPH oxidase homologs are required for normal cell differentiation and morphogenesis in Dictyostelium discoideum. Biochim Biophys Acta 1744:199–212. https://doi.org/10.1016/j.bbamcr.2005.02.004.
48. Webb JS, Givskov M, Kjelleberg S. 2003. Bacterial biofilms: prokaryotic adventures in multicellularity. Curr Opin Microbiol 6:578–585. https://doi.org/10.1016/j.mib.2003.10.014.
49. Gennaris A, Ezraty B, Henry C, Agrebi R, Vergnes A, Oheix E, Bos J, Leverrier P, Espinosa L, Szewczyk J, Vertommen D, Iranzo O, Collet JF, Barras F. 2015. Repairing oxidized proteins in the bacterial envelope using respiratory chain electrons. Nature 528:409–412. https://doi.org/10.1038/nature15764.
50. Kawahara T, Quinn MT, Lambeth JD. 2007. Molecular evolution of the reactive oxygen-generating NADPH oxidase (Nox/Duox) family of enzymes. BMC Evol Biol 7:109. https://doi.org/10.1186/1471-2148-7-109.
51. Krogh A, Larsson B, von Heijne G, Sonnhammer EL. 2001. Predicting transmembrane protein topology with a hidden Markov model: application to complete genomes. J Mol Biol 305:567–580. doi https://doi.org/10.1006/jmbi.2000.4315.
52. Sievers F, Wilm A, Dineen D, Gibson TJ, Karplus K, Li W, Lopez R, McWilliam H, Remmert M, Söding J, Thompson JD, Higgins DG. 2011. Fast, scalable generation of high-quality protein multiple sequence alignments using Clustal Omega. Mol Syst Biol 7:539. https://doi.org/10.1038/msb.2011.75.
53. Cowart RE, Singleton FL, Hind JS. 1993. A comparison of bathophenanthrolinedisulfonic acid and ferrozine as chelators of iron(II) in reduction

reactions. Anal Biochem 211:151–155. https://doi.org/10.1006/abio.1993.1246.
54. Maghzal GJ, Krause KH, Stocker R, Jaquet V. 2012. Detection of reactive oxygen species derived from the family of NOX NADPH oxidases. Free Radic Biol Med 53:1903–1918. https://doi.org/10.1016/j.freeradbiomed.2012.09.002.
55. Awai M, Narasaki M, Yamanoi Y, Seno S. 1979. Induction of diabetes in animals by parenteral administration of ferric nitrilotriacetate. A model of experimental hemochromatosis. Am J Pathol 95:663–673.
56. Ciccarelli FD, Doerks T, von Mering C, Creevey CJ, Snel B, Bork P. 2006. Toward automatic reconstruction of a highly resolved tree of life. Science 311:1283–1287. https://doi.org/10.1126/science.1123061.
57. Hancock JT, Jones OT. 1987. The inhibition by diphenyleneiodonium and its analogues of superoxide generation by macrophages. Biochem J 242:103–107. https://doi.org/10.1042/bj2420103.
58. Green TR, Wu DE. 1985. Detection of NADPH diaphorase activity associated with human neutrophil NADPH-O2 oxidoreductase activity. FEBS Lett 179:82–86.